Cement and Concrete Research 39 (2009) 659–663

Contents lists available at ScienceDirect

Cement and Concrete Research

journal homepage: http://ees.elsevier.com/CEMCON/default.asp

Sulfur speciation in granulated blast furnace slag: An X-ray absorption spectroscopic investigation

Amitava Roy *

J. Bennett Johnston, Sr., Center for Advanced Microstructures and Devices, Louisiana State University, Baton rouge, Louisiana 70806, USA

ARTICLE INFO

Article history:
Received 29 October 2008
Accepted 25 May 2009

Keywords:
Glass
Spectroscopy
Granulated blast furnace slag
Sulfate

ABSTRACT

Sulfur speciation in a granulated blast furnace slag (GGBFS) was analyzed by X-ray absorption near edge structure spectroscopy (XANES) before and after activation by saturated calcium hydroxide and five normal sodium hydroxide solutions. The solution to GGBFS ratio was 0.4.

XANES showed that sulfur in GGBFS existed mostly as sulfides (frozen in calcium polyhedra) with a minor amount as sulfate. A slowly-cooled blast furnace slag, in contrast, had most of the sulfide transformed to sulfate. After activation of GGBFS, more sulfate formed and crystalline sulfide phases became more apparent. More slag reacted at lower pH than at higher pH.

1. Introduction

Sulfur species, particularly in the sulfate form, exert an inordinately strong influence on the stability of cementitious materials even though they constitute a very small portion of the mass or volume. For example, the sulfate containing phase ettringite is implicated in sulfate attack in concrete and cement-stabilized soil, even though the amount of ettringite is low and the exact mechanism is not fully understood [1]. Radwan [2] noted that there was an optimum sulfide content for Egyptian GGBFS for Portland cement clinker, GGBFS, and gypsum mixtures for strength and other physical properties. These values decreased on both sides of the maximum. He suggested that these components be mixed in only those proportions which will keep the overall sulfide content down.

It is not easy to monitor the sulfur species in cementitious materials as it can be distributed among different phases and it can also be in the pore solution. Apart from the ettringite, the calcium silicate hydrate and monosulfate can contain some of the sulfate. In addition, some of the original sulfates phases such as gypsum and anhydrite may remain. If a sulfite sludge from a coal-fired power plant is used in some form of stabilization, the speciation of sulfur will be different [3]. Granulated blast furnace slag also has a different speciation for sulfur. Radwan [2] quoted Russian studies from the 1960s which showed that sulfide and sulfate are the main species of sulfur in GGBFS. Scott et al. [4] reported that a small amount of oldhamite (CaS) is a common occurrence in a group of 11 GGBFS from Britain and France. Oldhamite occurred both as independent dendritic crystals and inclusions in melilite. Van Dam et al. recently suggested that coarse slag aggregate (slowly-cooled blast furnace slag) can potentially supply sulfate for sulfate attack by oxidation of the calcium sulfide in it [5].

It is common knowledge that the interior of activated GGBFS (usually very light brown in color) assumes a green color when activated. The color is pale green within the first few hours and becomes darker over time. Scott et al. [4] reported metallic iron inclusions within melilite crystals and also as globules of immiscible iron, tens of micrometer in diameter. GGBFS is often used in waste stabilization with cementitious materials as it provides a reducing environment for the waste. Bajt et al. [6] showed by X-ray absorption spectroscopy that this environment reduced toxic hexavalent chromium to the more benign trivalent form. The iron content of GGBFS typically ranges from 0.2 to 1.6% (http://www.tfhrc.gov/hnr20/recycle/waste/GGBFS1.htm). The amount of iron as Fe_2O_3 in the GGBFS used in this study is 1.3%.

X-ray absorption spectroscopy is an element-specific analytical technique which can be used to study directly the speciation and oxidation state without any extensive wet chemical procedures. For example, the sulfide, sulfite and sulfate species in a sulfur-containing material can be easily identified and quantified by X-ray absorption near edge structure (XANES) spectroscopy [7] from the same specimen all at once. XANES focuses on the total sulfur, independent of exact speciation, or whether it is in crystalline, amorphous or aqueous form. In contrast, wet chemical methods would identify the species extracted in solution, not necessarily the species actually present in the solid sample. The objective of this study is to investigate speciation of sulfur in GGBFS and its changes after activation. The fate of sulfur speciation during slow cooling of slag was also studied.

---

* Tel.: +1 225 578 6706; fax: +1 225 578 6954.
E-mail address: reroy@lsu.edu.

0008-8846/$ – see front matter © 2009 Elsevier Ltd. All rights reserved.
doi:10.1016/j.cemconres.2009.05.007

2. Experimental procedure

2.1. Sample preparation

The slag used in the study was obtained from Buzzi Unicem. It was a 120 Grade slag. The slowly-cooled slag also came from the same source. The chemical composition of the slag is listed in Table 1. The sulfur content, however, was not provided. The typical sulfur (S) content of GGBFS is 1.4%, and ranges between 1.0 and 1.9%, as found by the National Slag Association from 18 analyses (http://www.tfhrc.gov/hnr20/recycle/waste/GGBFS1.htm).

The specimens for this study were prepared by weighing approximately 40 gm of slag in a Tri-pour™ polyethylene beaker and adding a solution so that a 0.4 solution to slag ratio was obtained. The solutions used were 5 N NaOH (pH 14.69), and saturated solutions of calcium hydroxide (pH ca. 12.6) [8,9]. (These conditions also simulate the pH in cementitious systems, including supersaturated pore water.) The slag and solution were thoroughly mixed with a stirrer, the beaker was covered with parafilm, and cured for required lengths of time. The mixes usually set within minutes to hours with the green color in the interior developing within hours of activation. The specimens were stored in air. After five months, the interior of most specimens was dark green while only a 1 to 2 mm thick light brown exterior shell remained. The data presented in this report came from specimens which were analyzed five months after preparation. The younger specimens showed very similar trends. The specimens were crushed to a fine powder with an agate mortar and pestle just before XANES measurements.

2.2. X-ray absorption spectroscopy

The sulfur K edge measurements were performed at the Double Crystal Monochromator beamline of the J. Bennett Johnston, Sr., Center for Advanced Microstructures and Devices (CAMD), Louisiana State University, Baton Rouge, Louisiana. The beamline operates in "windowless" mode, a 13-µm-thick Kapton™ window separating the experimental setup from the ring. The CAMD synchrotron ring operates at 1.3 GeV, with a typical ring current between 230 and 100 mA.

A thin layer of the finely-powdered sample was uniformly spread on a sulfur-free Kapton™ tape and placed in the chamber at 45° for fluorescence measurements and normal to the beam for transmission measurements.

The S K edge measurements were made with InSb 111 crystals. The resolution of the monochromator at this energy range is ca. 1 eV. The monochromator was detuned by 60% to remove the harmonics. The step sizes for measurements (with respect to the sulfur K edge, 2472.0 eV) were from −70 eV to −10 eV (1.5 eV steps), −10 eV to 30 eV (0.1 eV steps), and from 30 eV to 125 (1.5 eV steps); integration period was 2 s through all regions. The fluorescence X-rays were measured with a Canberra™ single-element germanium detector. S K edge measurements were made at the partial pressure of nitrogen 180 mTorr. The sulfur K edge was calibrated with the zinc sulfate hydrate ($ZnSO_4.2H_2O$) peak set at 2881.44 eV. The fluorescence spectra were collected repeatedly until good counting statistics were achieved. Data reduction was performed with Athena [10] and WinXAS [11].

The XANES standards used in the study were either reagent grade chemicals obtained from Alfa Aesar or Sigma Aldrich or naturally occurring minerals. These phases are typical sulfur-containing phases expected in construction materials. The source of each standard, their chemical formula, oxidation state of sulfur in them, and peak locations are given in Table 2.

Table 1
Chemical composition of GGBFS.

SiO_2	Al_2O_3	Fe_2O_3	CaO	MgO	K_2O	Na_2O
34.5	9.5	1.3	39.6	10.9	1.3	0.5

Table 2
XANES peaks of some selected sulfur compounds.

Phase/mineral	Peak position (eV)	Sulfur oxidation state	Source
Reagent grade gypsum ($CaSO_4 \cdot 2H_2O$)	2481.94	S^{+6}	Sigma-Aldrich
Reagent grade anhydrite ($CaSO_4$)	2481.9	S^{+6}	Alfa Aesar
Ettringite ($Ca_6[Al(OH)_6](SO_4)_3 \cdot 26H_2O$)	2481.89	S^{+6}	Prepared in the laboratory by CTL, Skokie, Ill.
Hannebachite ($CaSO_3$)	2471.13, 2477.45, 2481.59	S^{+4}	A mineral specimen of hannebachite from Hannebach, Eifel, Germany, was obtained through Roger's Minerals, Ontario, Canada.
Reagent grade calcium sulfide (oldhamite) (CaS)	2473.98, 2477.51	S^{-2}	Alfa Aesar
Sulfur	2472.71	S^0	Ward's Natural Science
Zinc sulfide (Sphalerite) (ZnS)	2473.32	S^{-2}	Ward's Natural Science

3. Results and discussion

3.1. Sulfur in granulated blast furnace slag

In XANES spectroscopy the strongest peak is known as the white line (Fig. 1, A). This peak is due to the resonance of the excited electron between 1s and np states. The subsequent peaks at higher energy are usually due to multiple scattering of the excited electron between different shells (for example, peaks B and C in Fig. 1). The absorption edge of sulfur shows a wide distribution depending on the oxidation state, −2 to +6, with the edge moving to higher energy with increasing oxidation state, spanning as much as 13 eV [12].

Fig. 1 shows the XANES spectra of sulfur and some sulfide phases. The absorption edge of sulfur (the first derivative) is at 2472.0 eV. Oldhamite (CaS), with sulfur oxidation state of −2, has the strongest peak (white line labeled A) at 2473.98 eV. The other minor peaks B, C and D occur at higher energies. Another sulfide phase, copper sulfide, is also included in the figure showing that when the sulfur is in the same oxidation state the peaks occur in the very similar energy range. The differences in peak intensities are due to the type of cation [13]. Fig. 2 shows the XANES spectra of gypsum, anhydrite, ettringite and

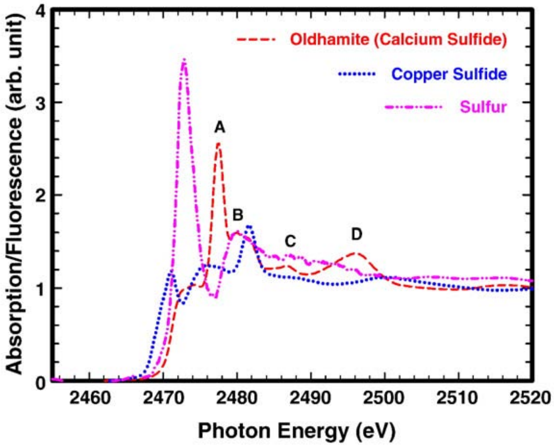

Fig. 1. Sulfur K edge XANES of sulfur and some sulfide minerals.

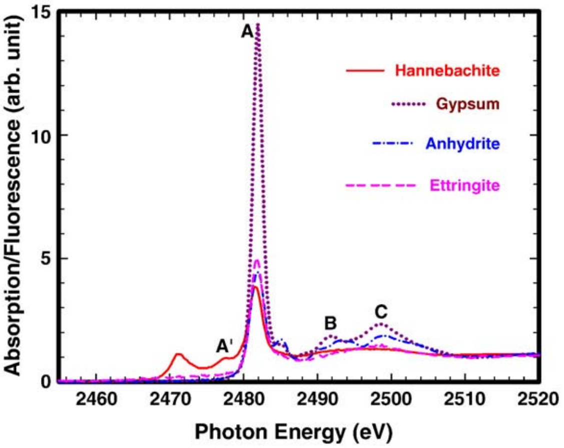

Fig. 2. Sulfur K edge XANES of some sulfite and sulfate minerals.

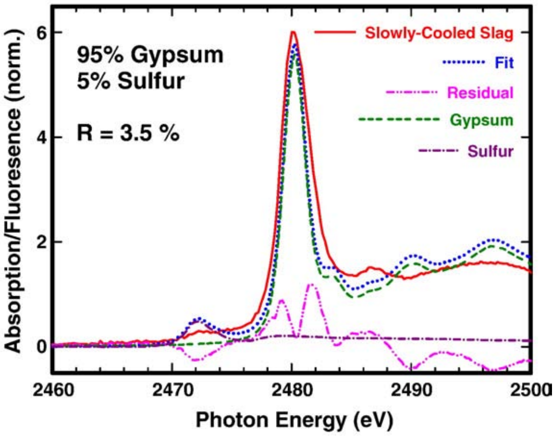

Fig. 4. Least squares fitting of slowly-cooled slag sulfur XANES spectrum.

hannebachite. Gypsum and anhydrite are important components of Portland cement and ettringite is a very important hydration product in such systems. Hannebachite is a by-product often found in the flue gas desulfurization sludge of coal-fired power plants. The hannebachite spectrum shown here, however, is unlike that of Pattanaik et al. [3] where the strong white line appears at 2478.0 eV. The hannebachite shown in Fig. 2, with sulfur in +4 oxidation state, has peaks at 2470.28 eV and 2481.62 eV, in addition to a peak at 2477.45 eV (Fig. 2, A'). The naturally occurring hannebachite specimen used in this study is thus not pure and contains sulfide and sulfate impurities. The sulfate peak in the gypsum, anhydrite, and ettringite occur around 2481.9 eV. Ettringite shows only a broad hump beyond the white line, in contrast to gypsum and ettringite (which show minor peaks B and C), as the sulfate ion in the ettringite structure is not directly bound to any cation [7].

Fig. 3 shows the XANES spectra of GGBFS from two batches and the spectrum of a slowly-cooled slag. The latter is included to show the sulfur speciation in the slag during slow cooling. X-ray diffractometry of the slowly-cooled slag showed (figure not included here) that it was mostly composed of calcium silicate larnite ($CaSiO_4$). No sulfate mineral could be positively identified. The amount of this sulfate phase is thus below the detection limit of X-ray diffractometry.

Fig. 4 shows least squares fitting results of the slowly-cooled slag XANES spectrum with the standards gypsum (95%) and sulfur (5%). Inclusion of calcium sulfide or anhydrite among the standards worsened the fit. The residual in Fig. 4 shows that the standards used are not the best possible ones. The sharp peak at 2480.10 eV of the slowly-cooled slag is due to the sulfate form (with sulfur in +6 oxidation state) as comparison with the gypsum and other sulfate spectra in the literature shows. However, this peak is quite broad compared to gypsum and the overall features of the slowly-cooled slag spectrum (for example, locations of peaks B (2486.64 eV) and C (2496.23 eV)) indicate that it is unlike any calcium sulfate. The presence of the peaks B and C suggests that the sulfate phase is quite crystalline in the slag. The sulfate in the slowly-cooled slag has a distinct pre-edge peak (2472.01 eV). The fit to native sulfur for this peak is only moderate at best, the residual being quite large. Phase diagram of the relevant system would suggest that this peak is due to a sulfide phase. If native sulfur is indeed present then reducing conditions are somehow arising which would lead to the breakdown of the sulfide to native sulfur. The presence of native sulfur is not necessarily deleterious as it is not going to get oxidized to produce sulfate species under ambient conditions. The use of sulfur as cement in concrete for certain environments, such as acidic, has been suggested. This subject has recently been reviewed [14].

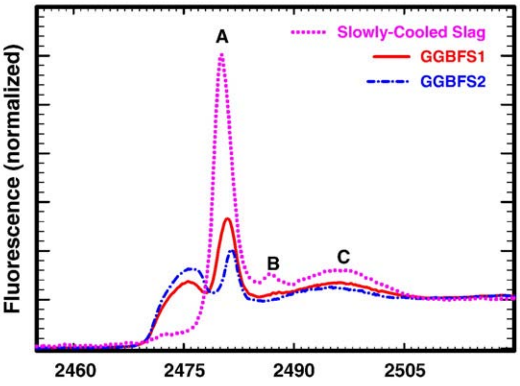

Fig. 3. Sulfur K edge XANES of GGBFS, with and without slow cooling.

Fleet et al. [15] investigated the role of sulfur in geologically-relevant glasses by melting silicate glasses with different amounts of sulfur. The glasses show broad sulfur peaks, some corresponding to oldhamite (CaS), added as a charge to these glasses to simulate natural compositions. It was [15] suggested that the broad peak of sulfur in glasses is due to its amorphous nature where the sulfur is “frozen” in different coordination to calcium (SCa_n polyhedra). Paris et al. [16] in their research related to sulfur in silicate magmas observed that sulfur exists in two states, sulfide and sulfate, the ratio depending on oxygen fugacity. According to them there is no intermediate state of sulfur (for example, sulfite). In some magmatic rocks, though the conditions were quite oxidizing, some sulfide persisted, probably due to locally reducing condition.

A comparison of the spectra shown in Fig. 3 with Figs. 1 and 2, and those from the literature, indicates that most of the sulfur in GGBFS is thus in amorphous form, with only a minor amount appearing as small crystallites [4]. Wet chemical analysis has suggested that sulfur in GGBFS, when it goes into solution, is mostly in polysulfide form [17]. The sulfur in the slowly-cooled slag is mostly in the sulfate state. Thus, as suggested by Van Dam and others [5], it is indeed possible for slag aggregate in concrete to be a source of sulfate for sulfate attack.

3.2. Sulfur in activated granulated blast furnace slag

Sulfur XANES spectra of GGBFS, activated by calcium hydroxide and sodium hydroxide, are shown in Figs. 5 and 6, respectively. The measurements came from small chips that were obtained from the dark green interior of the solidified mass and from the light brown exterior surface. (The chips were ground to fine powder before

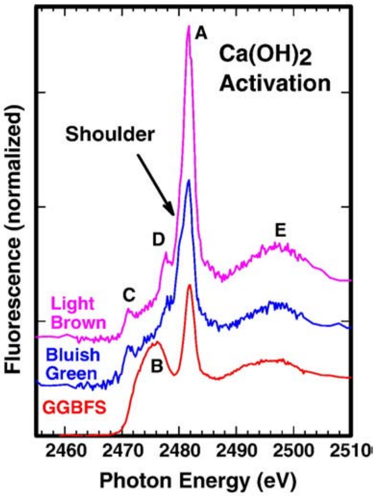

Fig. 5. Sulfur K edge XANES of GGBFS with calcium hydroxide activation.

measurement.) Fig. 7 shows the difference in the sulfur spectrum before and after hydration. The figures show that throughout the volume of the slag, after reaction, the sulfate content increases and the sulfide content decreases. The sulfate peak is more intense at lower pH (calcium hydroxide activation) than at higher pH (sodium hydroxide activation). At higher pH the reaction process is faster and thus possibly does not allow the release of "frozen" sulfide in GGBFS.

The broader sulfide peak of GGBFS in the range 2470 to 2480 eV is also reduced, followed by the appearance of some smaller, sharper peaks (C and D). One peak appears at a lower energy than the sulfide peak in the GGBFS itself. A perusal of the sulfide XANES spectra in the literature shows that the edge location depends on the type of cation and their coordination [13]. The sulfur is "exsolving" from the glass and forming distinct crystalline phases. The minor sulfide peaks C and D are more pronounced on the surface than in the interior. One possibility that these peaks are better visible is that the amorphous sulfur is reacting while the crystalline phases remain unchanged and become more visible over time. The peak D could be matched with oldhamite. The peak labeled E in Figs. 4, 5 and 6 is due to multiple scattering from surrounding shells [13].

A distinct shoulder is evident in the sulfate peak of the activated GGBFS on the low energy side in Figs. 5 and 6. Fig. 7 shows that this shoulder is due to the sulfate originally present in the slag that did not react. The shoulder is also more pronounced in the NaOH-activated slag than $Ca(OH)_2$-activated slag. This observation reconfirms the fact that the latter reacted more than the former.

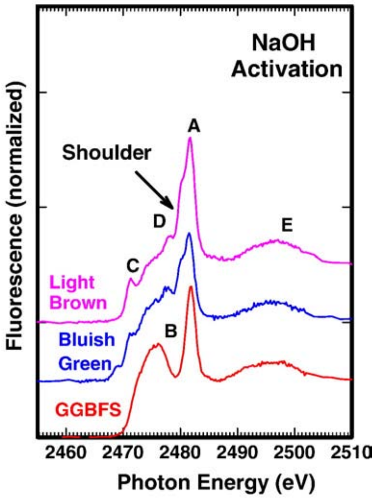

Fig. 6. Sulfur K edge XANES of GGBFS with sodium hydroxide activation.

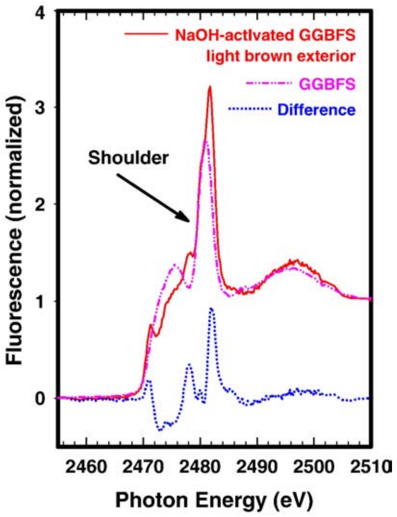

Fig. 7. Difference spectrum of GGBFS before and after sodium hydroxide activation.

4. Conclusions

Sulfur is present in GGBFS both as sulfide and sulfate, with the sulfide mostly in amorphous form. Slow cooling of the slag leads to almost complete conversion of the sulfide to sulfate. The sulfate phase, though crystalline, is unlike gypsum or anhydrite. The crystalline sulfide phases become more apparent after activation. More slag reacts at lower pH than at higher pH.

Acknowledgements

This article was developed from the project "Support Study for the Stability of Calcium Sulfate Base Course in a Wet Environment (736-99-1214)" funded by the Louisiana Transportation Research Center. The comments provided by the anonymous reviewers helped in improving the manuscript.

References

[1] C. Famy, H.F.W. Taylor, Ettringite in hydration of portland cement concrete and its occurrence in mature concretes, ACI Materials Journal 98 (4) (2001) 350–356.
[2] M.M. Radwan, Influence of the type of blast furnace slag on some characteristics of high slag cement, Silicates Industriels 67 (7–8) (2002) 89–95.
[3] S. Pattanaik, G.P. Huffman, S. Sahu, R.J. Lee, X-ray absorption fine structure spectroscopy and X-ray diffraction study of cementitious materials derived from coal combustion by-products, Cement and Concrete Research 34 (7) (2004) 1243–1249.
[4] P.W. Scott, S.R. Critchley, F.C.F. Wilkinson, The chemistry and mineralogy of some granulated and pelletized blastfurnace slags, Mineralogical Magazine 50 (355) (1986) 141–147.
[5] T.J. Van Dam, K.R. Peterson, L.L. Sutter, M.E. Housewright, Deterioration in concrete pavements constructed with slag coarse aggregate, Transportation Research Record 1834 (2003) 8–15.
[6] S. Bajt, S.B. Clark, S.R. Sutton, M.L. Rivers, J.V. Smith, Synchrotron X-ray microprobe determination of chromate content using X-ray-absorption near-edge structure, Analytical Chemistry 65 (13) (1993) 1800–1804.
[7] S.C.B. Myneni, in: C.N. Alpers, J.L. Jambor, D.K. Nordstrom (Eds.), X-ray and Vibrational Spectroscopy of Sulfate in Earth Materials, in Sulfate Minerals — Crystallography, Geochemistry and Environmental Significance, Mineralogical Society of America, Washington, D.C., 2000, pp. 113–172.
[8] P.J. Schilling, A. Roy, H.C. Eaton, P.G. Malone, W.N. Brabston, Microstructure, strength, and reaction-products of ground granulated blast-furnace slag activated by highly concentrated NaOH solution, Journal of Materials Research 9 (1) (1994) 188–197.
[9] A. Roy, P.J. Schilling, H.C. Eaton, P.G. Malone, W.N. Brabston, L.D. Wakeley, Activation of ground blast-furnace slag by alkali-metal and alkaline-earth hydroxides, Journal of the American Ceramic Society 75 (12) (1992) 3233–3240.

[10] B. Ravel, M. Newville, ATHENA, ARTEMIS, HEPHAESTUS: data analysis for X-ray absorption spectroscopy using IFEFFIT, Journal Of Synchrotron Radiation 12 (2005) 537–541.

[11] T. Ressler, WinXAS: a new software package not only for the analysis of energy-dispersive XAS data, Journal De Physique Iv 7 (C2) (1997) 269–270.

[12] F. Jalilehvand, Sulfur: not a “silent” element any more, Chemical Society Reviews 35 (12) (2006) 1256–1268.

[13] M.M. Fleet, XANES spectroscopy of sulfur in earth materials, The Canadian Mineralogist 43 (6) (2005) 1811–1838.

[14] A.M.O. Mohamed, M. El Gamal, Sulfur based hazardous waste solidification, Environmental Geology 53 (1) (2007) 159–175.

[15] M.E. Fleet, X.Y. Liu, S.L. Harmer, P.L. King, Sulfur k-edge XANES spectroscopy: chemical state and content of sulfur in silicate glasses, Canadian Mineralogist 43 (2005) 1605–1618.

[16] E. Paris, G. Giuli, M.R. Carroll, I. Davoli, The valence and speciation of sulfur in glasses by X-ray absorption spectroscopy, Canadian Mineralogist 39 (2001) 331–339.

[17] H. Satake, T. Hisano, S. Ikeda, The rapid-determination of sulfide, thiosulfate, and polysulfide in the lixiviation water of blast-furnace slag by means of argentimetric potentiometric titration, Bulletin of the Chemical Society of Japan 54 (7) (1981) 1968-1671.